TEST AND SIMULATION OF COMPOSITE SANDWICH STRUCTURE WITH A NOTCH UP TO FAILURE

O. Montagnier*[1,2], J.-P. Charles[3], G. Eyer[4], F. Mazerolle[2], N. Lahellec[3]

[1] *Centre de Recherche de l'Arme de l'air (CReA), EOAA, BA 701, F-13361 Salon air*
[2] *LMA, CNRS, UPR 7051, F-13402 Marseille Cedex 20, France*
[3] *LMA, Aix-Marseille Univ, CNRS, UPR 7051, F-13402 Marseille Cedex 20, France*
[4] *LMA, Aix-Marseille Univ, Centrale Marseille, CNRS, UPR 7051, F-13451 Marseille Cedex, France*
* *Corresponding Author: olivier.montagnier@inet.air.defense.gouv.fr*

Keywords: damage mechanics, experimental, notched structure, stress concentration, fracture, digital image correlation, glass/epoxy, sandwich structure,

Abstract

It is proposed a new test on a large sandwich notched specimen loaded in static bending/torsion and consisting of woven fabric GFRP laminates and foam material. The aim of this test is to generate crack initiation and propagation around the notch. This test is used to validate a model based on continuum damage mechanics and a nonlocal criterion developed since several years. Numerical results compared to DIC and the force at failure show the efficiency of the proposed approach.

1. Introduction

°The forecasting of composite material fracture is a challenge since many years. Many models have been developed in order to describe the multiple mechanisms leading to failure, such as matrix cracking, fiber/matrix debonding, transverse failure, delamination and fiber rupture mechanism. These models are generally identified on simple loading cases (tension, compression, 3 or 4 point bending, etc.) and simple geometries (beam, plate, etc). These tests try to minimize stress concentrations. However, it is necessary to evaluate their efficiency in a more complex situation, for example, on real structure or on experiment which resembles to a real structure. Here, it is proposed a new test on a large sandwich notched specimen, which looks like to an aeronautical structure (e.g. an helicopter blade), loaded in static bending/torsion. The aim of this test is to generate crack initiation and propagation around the notch.

This test is used to validate a model based on continuum damage mechanics (CDM) developed since several years [1, 2, 3, 4]. It accounts for the gradual diffuse damage induced by small cracks running parallel to the fiber direction [5]. The failure of woven ply laminated structures is obtained with a non-local ply scale criterion [2, 6, 4]. The model is implemented in ABAQUS.

The first part of this paper describes the model: CDM and non-local ply scale criterion. Then the experiment is presented. Finally, the numerical results compare to the experimental results, obtained via digital image correlation (DIC), show the efficiency of the method.

2. Continuum damage mechanics of woven ply

The model proposed is based on CDM. It describes directly the mechanical behavior of the composite material on the ply scale (meso-model). The processes occurring at the micro-scale are described via thermodynamic expressions. In order to obtain a general model, the woven ply is modelled as a [0°,90°] laminate constituted of UD plies [4]. For example, the specimen was constituted of glass/epoxy unbalanced woven plies with 83% in the warp direction and 17% in the weft direction. Then, the laminate consisting of two identical UD plies. The first ply is oriented at 0°and has a thickness amounting to 83% of the whole woven ply thickness. The second ply is oriented at 90°and has a thickness amounting to 17% of the whole woven ply thickness.

2.1. Damage behavior of UD ply

The damage is only considered in the plane of the ply and assumed to be uniform throughout the thickness of the ply. It is expressed in terms of loss of stiffness

$$E_1 = E_1^0(1-d_1)\ ;\ E_2 = E_2^0(1-d_2)\ ;\ G_{12} = G_{12}^0(1-d_{12}) \quad \text{with} \quad \{d_1, d_2, d_{12}\} \in [0,1] \tag{1}$$

where d_1, d_2 and d_{12} are the damage in axial, in transverse and in shear directions, respectively. These damage variables are initially null then E_1^0, E_2^0 and G_{12}^0 are initial stiffness in axial, in transverse and in shear directions, respectively. Assuming that we are dealing with plane stresses and small perturbations assumptions, the local strain energy of each ply can be written in terms of stresses as follows [5]

$$\mathrm{E} = \frac{1}{2}\left(\frac{\langle\sigma_1\rangle_+^2}{E_1^0(1-d_1)} + \frac{\langle\sigma_1\rangle_-^2}{E_1^0} + \frac{\langle\sigma_2\rangle_+^2}{E_2^0(1-d_2)} + \frac{\langle\sigma_2\rangle_-^2}{E_2^0} - 2\frac{\nu_{12}^0}{E_1^0}\sigma_1\sigma_2 + \frac{\sigma_{12}^2}{G_{12}^0(1-d_{12})}\right) \tag{2}$$

where $\langle.\rangle_+$ and $\langle.\rangle_-$ stand for positive part and negative part. Noting that there is no damage during compressive steps. Thermodynamic forces associated to internal variables can be deduced from strain energy

$$Y_{d_j} = \frac{\partial \mathrm{E}}{\partial d_j} = \frac{\left\langle\sigma_j\right\rangle_+^2}{2E_j^0\left(1-d_j\right)^2} \quad j \in \{1,2\}\ ; \quad Y_{d_{12}} = \frac{\partial \mathrm{E}}{\partial d_{12}} = \frac{\sigma_{12}^2}{2G_{12}^0(1-d_{12})^2} \tag{3}$$

The development of internal variables depends on these thermodynamic forces or more specifically, on their maximum values during the loading history. In the fiber direction, the brittle fracture is described with a threshold model

$$d_1 = 0 \quad \text{if} \quad Y_{d_1} < Y_{d_1}^{\max} \quad \text{else} \quad d_1 = 1 \tag{4}$$

The damage in the transverse direction is based on a statistic law [3]

$$d_2 = \left\langle 1 - \mathrm{e}^{-\left(Y_{eq}-Y_0\right)}\right\rangle_+ \quad \text{with} \quad \dot{d}_2 \geq 0 \tag{5}$$

where $Y_{eq} = aY_{d_2}^m + bY_{d_{12}}^n$ is an equivalent thermodynamic force that accounted for the coupling mechanism between damage in transverse and shear direction. The damage mechanisms like matrix micro-cracking decrease the transverse and shear stiffness at the same time. Accordingly, the damage in shear direction is assumed to be proportional to the previous one

$$d_{12} = cd_2 \tag{6}$$

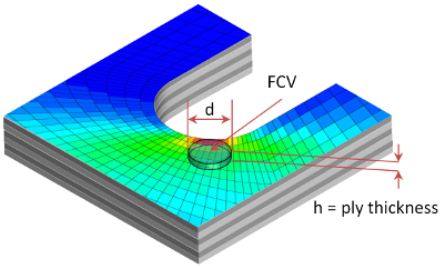

Figure 1. Fracture characteristic volume (FCV) at the edge of a notch

2.2. Inelastic strain of UD ply

Inelastic strains were observed in case of $[45]_8$ laminate in [3]. Here, only the inelastic strains in the shear direction is taken into account. The coupling between damage and plasticity is accounted for in terms of the effective stress and the effective strain [5]

$$\tilde{\sigma}_{12} = \frac{\sigma_{12}}{1 - d_{12}} \quad \text{and} \quad \dot{\tilde{\varepsilon}}^p_{12} = \dot{\varepsilon}^p_{12}(1 - d_{12}) \tag{7}$$

A kinematic linear hardening model is used to describe these strains where it is assumed that the stresses σ_1 and σ_2 has no effect

$$f = \left|\tilde{\sigma}_{12} - C_0\tilde{\varepsilon}^p_{12}\right| - R_0 \tag{8}$$

where R_0 is the initial inelastic strain threshold and C_0 is the linear law coefficient.

2.3. Nonlocal criterion

In paper [2], it was observed that local criterion underestimate strongly the force at failure on quasi-isotropic laminated structures (plate with a hole). Whitney and Nuismer [7] have also pointed out the effect of stress concentration and proposed the two well-known Point Stress and Average Stress Methods. However, these methods are not easy to use, especially because the characteristic length depends on the material as well as on the geometry of the specimen. We therefore developed an approach based on a Fracture Characteristic Volume (FCV) (see Fig. 1). We use the value of the averaged stress in the fiber direction in the following form

$$d_1 = 0 \quad \text{if} \quad \bar{\sigma} = \frac{1}{V}\int \sigma dV < \sigma_f^{\max} \quad \text{else} \quad d_1 = 1 \quad \text{with} \quad V = t \times S \tag{9}$$

where $\sigma_f^{\max}$ is the stress at failure in the fiber direction (identified in a tensile test), t is the ply thickness and S is the characteristic surface. The identification of the characteristic surface and implementation of the method in the ABAQUS software is given in [2, 6].

3. Specimen and experimental setup

The sandwich specimen (925mm x 340mm x 21mm) and the loading is inspired by helicopter composite blade geometry and loading (Fig. 2). In particular, the stacking sequence of the face notched (40mm x 1mm) is [±45°]. A tensile force is applied on a lever arm positioned at the top of the specimen to obtain a coupled bending/torsion load. The bottom is clamped.

The specimen geometry and the stacking sequence allow to prevent the specimen from fracture at the clamped end, local buckling and delamination at the lateral edge of the specimen in order

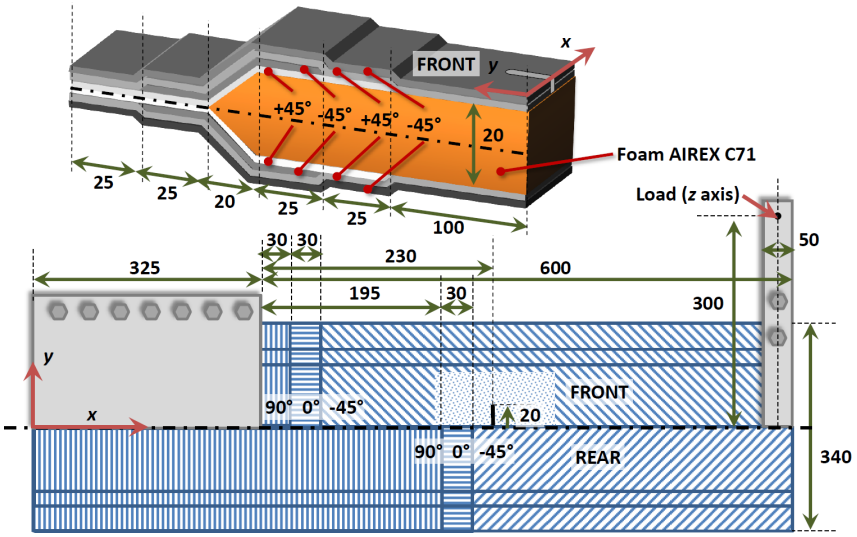

Figure 2. Specimen geometry, test geometry and stacking sequence

to focus crack initiation. The front face was reinforced with 0°and 90°plies near the clamped end. The rear face, mainly in compression during the test, was reinforced with 0°and 90°plies to guarantee that no local buckling occurred. The two faces of the specimen were jointed and reinforced with +45°and -45°plies.

The specimen was manufactured in two step. During the first step, only the front face was wrapped on the foam. The material unbalance generates a stacking sequence unbalanced ([±45°]) which generates some twist of the half-specimen. This effect is counterbalanced during the manufacture of the second face. In the future, balanced woven plies will be used to avoid this effect.

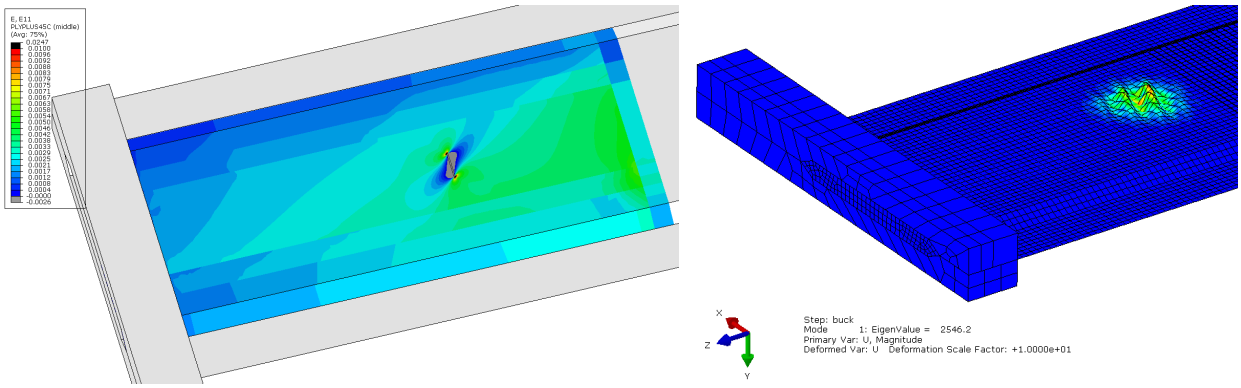

(a) Front face: strain in the fiber direction of the 45°ply (elastic model) (b) Rear face: first buckling mode on the fine mesh model

Figure 3. Finite element simulation of the experiment

Before the test, the entire specimen was modeled in ABAQUS using the classical laminate theory. The computation permits to estimate a crack initiation for a load of about 100daN (Fig. 3 (a)). Noting that the effect of the foam was insignificant in this computation and was not take into account. The results of the buckling simulation (linear perturbation) are given in Fig. 3 (b) and Tab 1. They shown a margin of about 2.5 comparatively to the fracture load. Noting that in this case, the effect of the foam was significant in the computation.

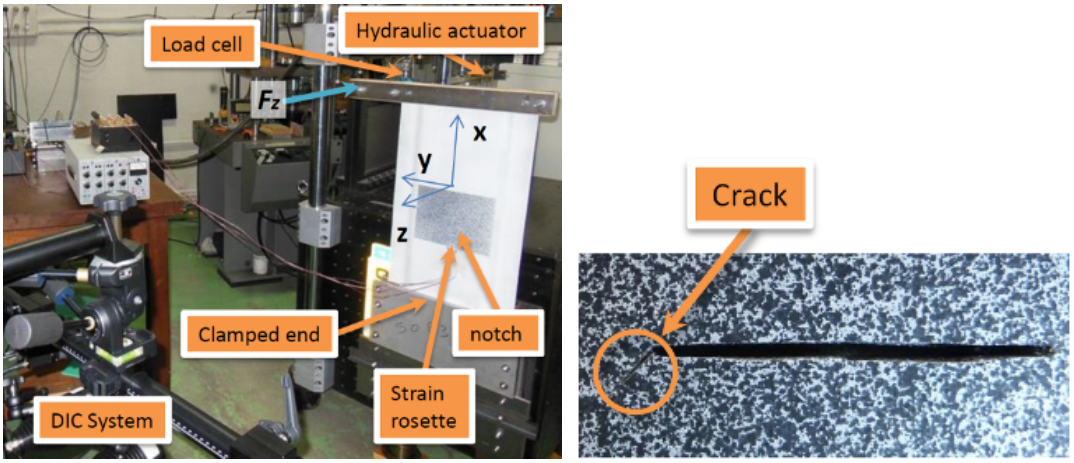

(a) (b)

Figure 4. (a) Experimental setup ; (b) Crack propagation at 45°at the end of the test

Mesh		**Large**	**Medium**	**Fine**
Number of elements	-	4500	11 700	27 600
Buckling load	daN	285	267	254

Table 1. Convergence of the buckling load vs. the number of finite elements

The experimental setup is presented on the Fig. 4 (a). During the test, the strains around the notch were measured with 3D DIC (ARAMIS software). Locally, a strain gage rosette was used to verify the strains obtained with DIC. The tension load F was applied with an hydraulic actuator and measured with a load cell. The direction of the load (**z** axis) was assumed to be constant. The crack initiation was observed for $F = 104$ daN. Then, the crack propagation at -45°was stable (see Fig. 4 (b)) until the end of the test when $F = 120$ daN.

4. Comparison between test and simulation

To simplified the comparison between experiment and simulation, only the area measured with DIC was computed in ABAQUS. Only the front laminate of the sandwich was modeled and plane stress state was assumed. The displacement field issued from DIC is applied to the edge of the model. The assumption that the displacement field at the outer surface corresponds to the displacement of the middle surface was made. The computation includes damage and plasticity. By using the maximum stress criterion ($\sigma^{\max}_{f_{UD}} = 960$ MPa) to describe the first ply failure, we underestimate the force at failure by a factor of 3.5 ($F_{\max} = 30$ daN). The nonlocal criterion gives a force at failure of 96 daN quasi similar to the force measured in the experimental test.

The simulation (for the outer surface of the laminate) and the DIC is given in Fig. 5. The step presented for the DIC corresponds to the strain field before crack initiation and for the simulation to the strain field when the non-local criterion gives the rupture of the laminate. It is important to note that the DIC gives the strain field from the outer surface of the specimen, mainly constituted of warp fibers (83%) at -45°. On the other hand, Fig. 4 (b) show that the crack propagation (at -45°) is piloted by the fiber fracture in the warp fibers at +45°(inner surface). It is not possible to obtain directly the strain in this ply but if the curvatures are smalls, the transverse strain in the -45°ply corresponds to the longitudinal strain in the the 45°ply. In Fig. 5, longitudinal strain (scale between -0.3% and 0.3%), transverse strain (scale between 0% and 1%) and shear strain fields (scale between -3% and 3%) obtained with the simulations

correlates well with the DIC. In particular, the transition between 2 and 3 plies in the staking sequence is highly visible. A more precise comparison can be observed in Fig. 6. If we note that the area where the DIC is not computed is larger than the size of the notch, it can be observed that the strain field is very similar. This field near the notch are plotted along the section 1 and 2 in Fig. 7 (a) and the same conclusion can be made. Far from the stress concentration at the edge of the notch (at point 1), force versus strain curve is compared to the linear and non linear model (Fig. 7 (b)). The damage field is given in Fig. 8 (a) showing a large area with damage near to 1. Finally, the computed longitudinal stress is plotted along the section 1 in the Fig. 8 (b). It can be observed that the longitudinal stress is 3.5 times higher than the longitudinal stress at failure in tension for the linear model and 6 times for the non linear model. It show the interest of the nonlocal criterion. In particular, we note that the stress gradient is twice in the case of the non linear model.

5. Conclusion

In this paper, it is proposed a new test on a large sandwich notched specimen loaded in static bending/torsion and consisting of woven fabric GFRP laminates and foam material. The aim of this test is to generate crack initiation and propagation around the notch. This test is used to validate a model based on continuum damage mechanics and a nonlocal criterion developed since several years. Numerical results compared to DIC and the force at failure show the efficiency of the proposed approach.

References

[1] Ch Hochard, P-A Aubourg, and J-P Charles. Modelling of the mechanical behaviour of woven-fabric cfrp laminates up to failure. *Composites Science and Technology*, 61(2):221–230, 2001.

[2] Christian Hochard, Noël Lahellec, and Cyril Bordreuil. A ply scale non-local fibre rupture criterion for cfrp woven ply laminated structures. *Composite Structures*, 80(3):321–326, 2007.

[3] Y Thollon and Ch Hochard. A general damage model for woven fabric composite laminates up to first failure. *Mechanics of Materials*, 41(7):820–827, 2009.

[4] Stéphanie Miot, Ch Hochard, and Noël Lahellec. A non-local criterion for modelling unbalanced woven ply laminates with stress concentrations. *Composite Structures*, 92(7):1574–1580, 2010.

[5] P. Ladevèze and E. Le Dantec. Damage modelling of the elementary ply for laminated composites. *Composites Science and Technology*, 43(3):257–267, 1992.

[6] C. Hochard, S. Miot, N. Lahellec, F. Mazerolle, M. Herman, and JP Charles. Behaviour up to rupture of woven ply laminate structures under static loading conditions. *Composites Part A*, 40(8):1017–1023, 2009.

[7] J Ma Whitney and RJ Nuismer. Stress fracture criteria for laminated composites containing stress concentrations. *Journal of Composite Materials*, 8(3):253–265, 1974.

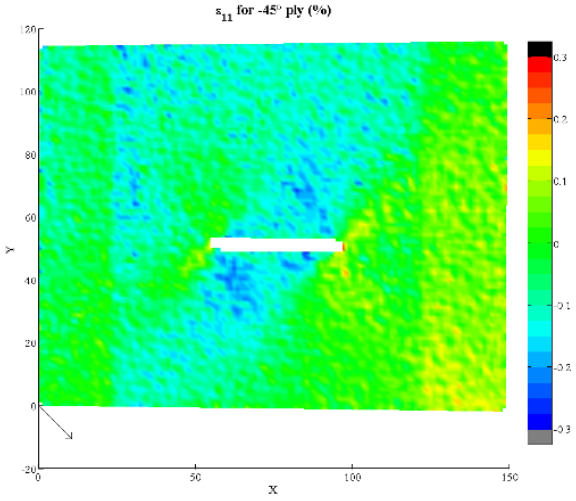

(a) ARAMIS : longitudinal strain of the -45°ply

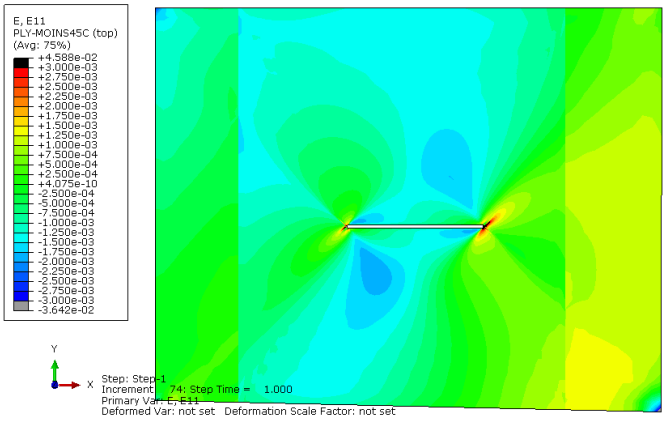

(b) ABAQUS : longitudinal strain of the -45°ply

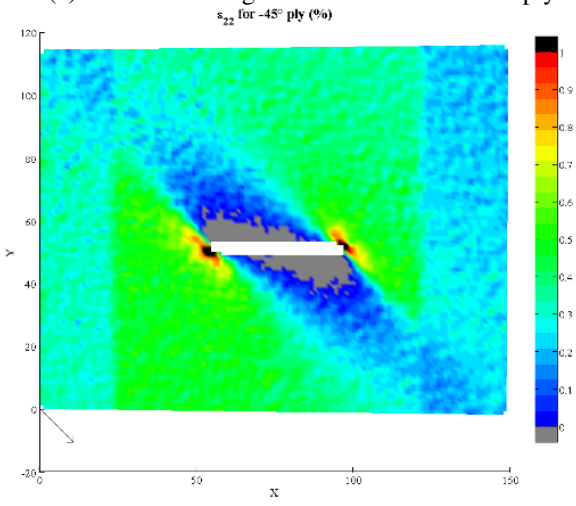

(c) ARAMIS : transverse strain of the -45°ply

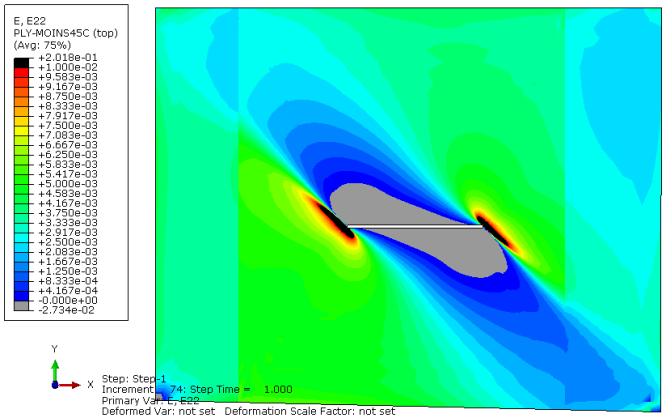

(d) ABAQUS : transverse strain of the -45°ply

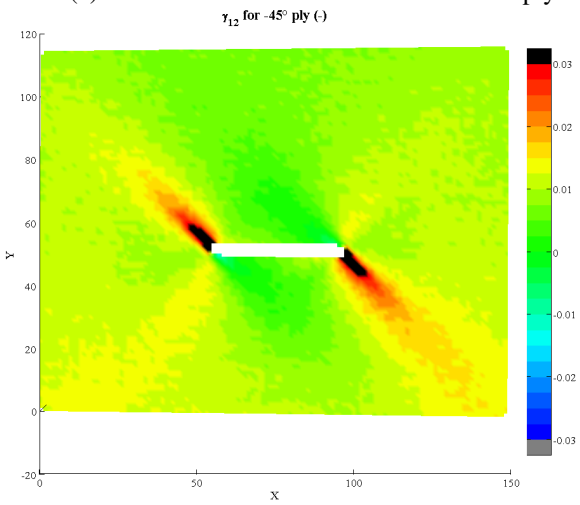

(e) ARAMIS : plane shear strain of the -45°ply

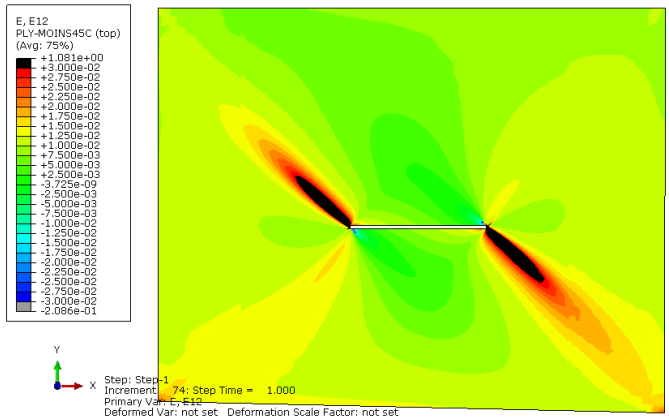

(f) ABAQUS : plane shear strain of the -45°ply

Figure 5. Comparison of strain field at the outer surface of the specimen (strain in %)

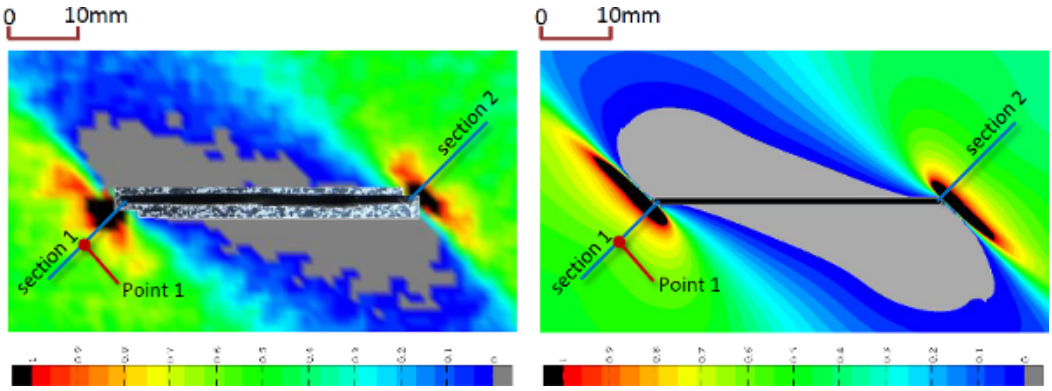

(a) ARAMIS (b) ABAQUS

Figure 6. Normal strain field in the (**x** + **y**) direction around the notch before crack initiation (in %)

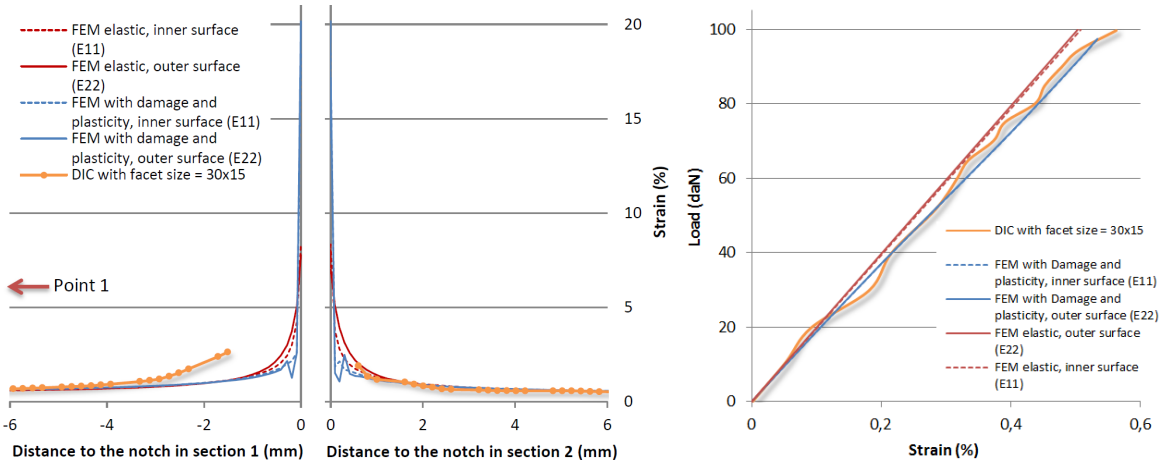

(a) along section 1 and 2, before crack initiation (b) time evolution at point 1

Figure 7. Evolution of the normal strain in the (**x** + **y**) direction around the notch

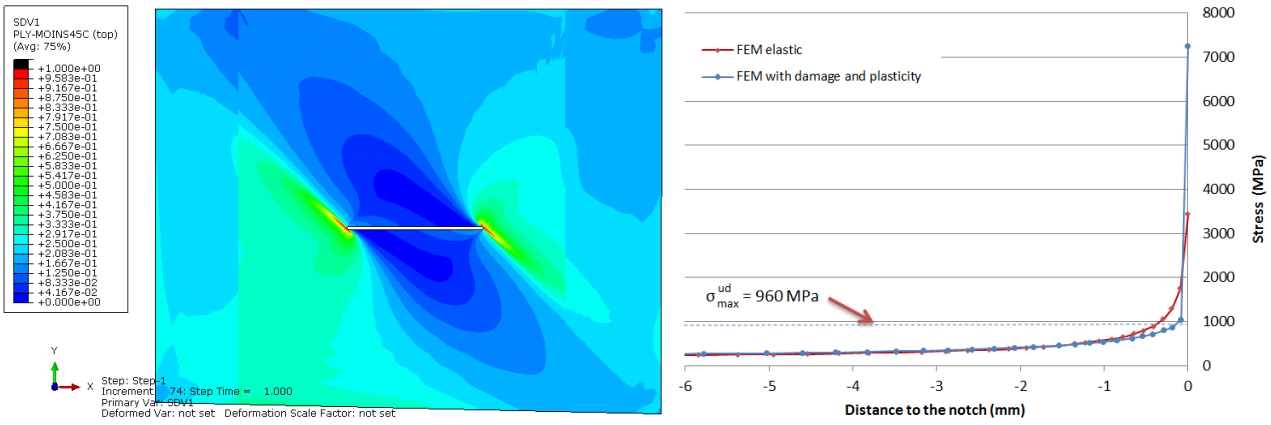

(a) damage field in the -45°ply ($d_2 = d_{12}$) (b) longitudinal stress in the +45°ply along section 1

Figure 8. Effect of the damage on the stress field